

UNCLASSIFIED

AD 285 506

*Reproduced
by the*

**ARMED SERVICES TECHNICAL INFORMATION AGENCY
ARLINGTON HALL STATION
ARLINGTON 12, VIRGINIA**



19990518132

UNCLASSIFIED

NOTICE: When government or other drawings, specifications or other data are used for any purpose other than in connection with a definitely related government procurement operation, the U. S. Government thereby incurs no responsibility, nor any obligation whatsoever; and the fact that the Government may have formulated, furnished, or in any way supplied the said drawings, specifications, or other data is not to be regarded by implication or otherwise as in any manner licensing the holder or any other person or corporation, or conveying any rights or permission to manufacture, use or sell any patented invention that may in any way be related thereto.

Ad No. 285506

STANDARD COPY

285506

**AVCO
EVERETT**

①

2790

**RESEARCH
LABORATORY**

a division of
AVCO CORPORATION

**CALCULATION OF HEAT TRANSFER
FROM SIMILARITY BOUNDARY LAYER
EQUATIONS BY A SIMPLE INTEGRAL METHOD**

Nelson H. Kemp

**RESEARCH REPORT 137
Contract No. AF 04(694)-33
June 1962**

prepared for
**HEADQUARTERS
BALLISTIC SYSTEMS DIVISION
AIR FORCE SYSTEMS COMMAND
UNITED STATES AIR FORCE**

3.60

60718 1962

19990518132

TDA

**CALCULATION OF HEAT TRANSFER
FROM SIMILARITY BOUNDARY LAYER
EQUATIONS BY A SIMPLE INTEGRAL METHOD**

by

Nelson H. Kemp

**AVCO-EVERETT RESEARCH LABORATORY
a division of
AVCO CORPORATION
Everett, Massachusetts**


Contract No. AF 04(694)-33

June 1962


prepared for

**HEADQUARTERS
BALLISTIC SYSTEMS DIVISION
AIR FORCE SYSTEMS COMMAND
UNITED STATES AIR FORCE
Air Force Unit Post Office
Los Angeles 45, California**

SUMMARY

 A simple integral method is developed for calculation of the heat transfer rate from similarity boundary layer equations with arbitrary variation of fluid properties. The method is applied to the end wall of a shock tube behind a reflected shock in a perfect gas, and to the stagnation point for a gas in thermodynamic equilibrium with Lewis number unity. Explicit formulas and results are obtained when the fluid properties are powers of the enthalpy or temperature, and the Prandtl number is constant.

For the end wall geometry, an analytical expression for the heat transfer rate is derived which can be correlated with exact calculations within $\pm 3\%$ for all cases compared.

For the stagnation point geometry, two pair of transcendental algebraic equations are obtained, one pair of which gives the heat transfer rate when the momentum layer is thinner than the energy layer, the other pair when it is thicker. Numerical solutions of these equations, ~~requiring needless computing time through integration of the exact differential equations,~~ can be correlated with exact solutions to within $\pm 4\%$. The integral method indicates the pressure gradient parameter and Prandtl number can be combined into only one parameter and examination of results of exact calculations shows this correlation to be quite accurate. 

NOTATION

A	constant of integration, Eq. (3.20)
c_p	specific heat per unit mass
\bar{c}_p	frozen specific heat per unit mass of gas mixture
f	dimensionless stream function, Eq. (3.8)
g	dimensionless total enthalpy, Eq. (3.8)
H	total enthalpy
I	integral expression, Eq. (3.25)
I_n^f	Eq. (3.40)
I_n^g	Eq. (3.42)
j	index of dimensionality, = 1 for axisymmetric flow = 0 for two-dimensional flow
K	ρk
k	thermal conductivity (frozen, in the case of an equilibrium gas)
N	distance from edge of energy boundary layer, Eq. (3.31)
p	pressure
$-q_w$	heat transfer rate to surface
T	absolute temperature
t	time
u	velocity component parallel to surface
v	velocity component normal to surface
x	coordinate parallel to surface
y	coordinate normal to surface
η	similarity variable, Eqs. (2.7) and (3.11)

- θ non-dimensional temperature, Eq. (2.8)
 κ $\rho k / \bar{c}_p$
 λ, ν exponents in thermal conductivity expression, Eq. (2.22)
 μ viscosity
 ρ mass density
 σ Prandtl number $\bar{c}_p \mu / k$
 ϕ_1, ϕ_2 heat flux potentials for end wall, Eq. (2.11), and stagnation point, Eq. (3.17), respectively
 χ_1, χ_2 functions in the definition of the similarity variable for end wall, Eq. (2.5), and stagnation point, Eq. (3.7), respectively
 ω exponent in thermal conductivity expression for end wall, Eq. (2.17), and $\rho k / \bar{c}_p$ expression for stagnation point, Eq. (3.37)

Subscripts

- c** break in k vs T curve
e edge of boundary layer
f edge of momentum layer
g edge of energy layer
o reference condition
w surface condition
st stagnation point

SECTION 1

INTRODUCTION

Many of the heat transfer boundary layer problems of interest in connection with high-speed missile and space vehicle flight, as well as related laboratory configurations, involve similarity solutions of the boundary layer equations. Examples are the stagnation point, the end wall of a shock tube, and the constant-pressure flows along cones, wedges, and side walls of shock tubes. Similarity solutions are also important as the building blocks of the "local-similarity" method of approximate boundary layer computation, which has come into wide use in recent years.

The usefulness of the similarity equations is associated with the fact that they represent a reduction of partial differential equations in two variables to ordinary differential equations, thus facilitating immensely the numerical work needed to obtain solutions. Another method of performing this reduction to ordinary differential equations has long been used in boundary layer theory -- the Karman-Pohlhausen method. In this technique, the partial differential equations are integrated once in a direction normal to the surface, leaving ordinary differential equations involving integrals of the dependent variables such as velocity, temperature, etc. Profiles for these quantities are assumed and inserted in the integrals, enabling evaluation of the coefficients of the ordinary differential equations.

The idea of this paper is to combine the two techniques, treating the ordinary differential equations of similarity theory by the Pohlhausen integral method, and so arriving at an expression for the heat transfer rate to the surface involving only simple quadratures. This application of integral methods to ordinary differential equations has been used before in some special cases. The incompressible momentum equation for the flat plate and the two-dimensional stagnation point are discussed in Schlichting's textbook.¹ Bush² uses it on the similar compressible boundary layer equations for the case where the product of density and viscosity is constant and the Prandtl number is unity. It is our object here to develop the method for arbitrary fluid property variations (with examples worked out for power law variations) with an eye toward later application to heat transfer problems involving dissociated and ionized gases.

The basis of the method is the representation of the temperature (or enthalpy) profile as a function of the similarity variable by an expression which is simple enough to be easily integrable, yet which leads to values for the heat transfer which are sufficiently accurate. The profile used here was first suggested by Jepson,³ who obtained a remarkably accurate formula for heat transfer to a flat plate at Prandtl number zero, with the thermal conductivity an arbitrary power of the temperature. It was this work which

stimulated the developments described in the present report.

Two cases will be discussed to illustrate the method of solution the similarity equations. The first is the heat transfer from a perfect gas to the end wall of a shock tube; the second is the heat transfer from a gas in thermodynamic equilibrium with Lewis number unity to a stagnation point. When power law fluid properties are used, the first case leads to a simple algebraic formula for heat transfer rate; and the second leads to a pair of transcendental algebraic equations that can be solved much more quickly than the similarity differential equations, which require the integration of a two-point boundary value problem.

There is no treatment in this report of cases where the energy equation is coupled to continuity equations for various species in the gas, as would be the case in a dissociating or ionizing gas which did not fulfill the conditions of thermodynamic equilibrium and Lewis number unity. However, extension of the method to this situation is under investigation and will be the subject of future reports.

The author would like to acknowledge the frequent advice and encouragement of Prof. James A. Fay during the course of the work reported here. The machine computations were carried out by Mr. Richard Goodman and Miss Patricia Jackson.

SECTION 2

END WALL HEAT TRANSFER

Between the end wall of a shock tube and the reflected shock which recedes from it there is a sample of hot gas which, neglecting boundary layer displacement effect, is stationary. Being in contact with the cold wall, the gas is cooled by a temperature boundary layer growing from the wall. This is a Rayleigh-type problem, since it can be represented by a cold wall suddenly put in contact with a hot, quiescent gas sample. If the gas were treated as incompressible, we would expect the solution to depend on the usual similarity variable of Rayleigh problems, y/\sqrt{t} , where y is distance normal to the wall. Because of compressibility, we expect that this variable is modified by the Howarth transformation to $\int \rho dy/\sqrt{t}$.

Let us first consider a perfect gas with no dissociative or ionizing effects. There is no flow parallel to the wall (in the x direction) nor are there any derivatives in this direction. The continuity, normal momentum and energy equations are

$$\frac{\partial \rho}{\partial t} + \frac{\partial \rho v}{\partial y} = 0 \quad (2.1a)$$

$$\rho \left(\frac{\partial v}{\partial t} + v \frac{\partial v}{\partial y} \right) = - \frac{\partial p}{\partial y} + \frac{4}{3} \frac{\partial}{\partial y} \left(\mu \frac{\partial v}{\partial y} \right) \quad (2.1b)$$

$$\rho c_p \left(\frac{\partial T}{\partial t} + v \frac{\partial T}{\partial y} \right) = \frac{\partial}{\partial y} \left(k \frac{\partial T}{\partial y} \right) + \frac{\partial p}{\partial t} + v \frac{\partial p}{\partial y} + \frac{4}{3} \mu \left(\frac{\partial v}{\partial y} \right)^2 \quad (2.1c)$$

The continuity equation indicates that density changes lead to velocities normal to the wall. When the usual boundary layer order of magnitude arguments are applied to these equations (2.1b) tells us that $p = p_e + O(\delta^2)$ where p_e is the pressure external to the boundary layer, so that the pressure terms in (2.1c) can be ignored. The dissipation term in (2.1c) is of order $\mu = O(\delta^2)$ also, and thus also negligible. The boundary layer energy equation then becomes

$$\rho c_p \left(\frac{\partial T}{\partial t} + v \frac{\partial T}{\partial y} \right) = \frac{\partial}{\partial y} \left(k \frac{\partial T}{\partial y} \right) \quad (2.2)$$

This combined with the continuity equation (2.1a) and an equation of state serve to define the temperature and flow field. The boundary conditions are:

$$y=0: \quad v=0, \quad T=T_w = \text{constant} \quad (2.3a)$$

$$y=\infty: \quad T=T_e = \text{constant} \quad (2.3b)$$

The velocity v can be eliminated by use of the continuity equation (2.1a). This enables us to write the convective derivative operator as

$$\rho \left(\frac{\partial}{\partial t} + v \frac{\partial}{\partial y} \right) = \rho \frac{\partial}{\partial t} - \left(\frac{\partial}{\partial t} \int_0^y \rho dy \right) \frac{\partial}{\partial y} \quad (2.4)$$

We now introduce the similarity variable by

$$\eta \equiv \chi_1(t) \int_0^y \rho dy \quad (2.5)$$

and assume that T and ρ depend on η alone. If η is then inserted into (2.4) and (2.2), the result is

$$\frac{d}{d\eta} \left(\frac{\rho k}{\rho_0 k_0} \frac{dT}{d\eta} \right) + \left(\frac{1}{\chi_1} \frac{d}{dt} \frac{1}{\chi_1} \frac{c_{p0}}{\rho_0 k_0} \right) \frac{c_p}{c_{p0}} \eta \frac{dT}{d\eta} = 0 \quad (2.6)$$

where the subscript 0 refers to quantities evaluated at same reference condition to be chosen later. The quantity χ_1 is chosen to make the expression in parenthesis in the second term equal to unity, yielding

$$\eta = \left(2t \rho_0 k_0 / c_{p0} \right)^{-1/2} \int_0^y \rho dy \quad (2.7)$$

If we further non-dimensionalize T with the external temperature T_e , the final equation we must solve is

$$\frac{d}{d\eta} \left(\frac{K}{K_0} \frac{d\theta}{d\eta} \right) + \frac{c_p}{c_{p0}} \eta \frac{d\theta}{d\eta} = 0, \quad \theta \equiv \frac{T}{T_e}, \quad K \equiv \rho k \quad (2.8)$$

with the boundary conditions

$$\theta(0) \equiv \theta_w = T_w/T_e, \quad \theta(\infty) = 1 \quad (2.9)$$

The heat transfer rate to the wall can be written with the help of (2.7) as

$$-q_w = k_w \left(\frac{\partial T}{\partial y} \right)_w = \left(\frac{\rho_0 k_0 c_{p0}}{2t} \right)^{1/2} T_e \left(\frac{K}{K_0} \frac{d\theta}{d\eta} \right)_w \quad (2.10)$$

We see that a heat flux potential ϕ_1 , may be defined by

$$\frac{d\phi_1}{d\eta} \equiv \frac{K}{K_0} \frac{d\theta}{d\eta}, \quad \phi_1 - \phi_{1,w} = \int_{\theta_w}^{\theta} \frac{K}{K_0} d\theta \quad (2.11)$$

such that the heat transfer rate to the wall is

$$-q_w = \left(\frac{\rho_0 k_0 c_{p0}}{2t} \right)^{1/2} T_e \left(\frac{d\phi_1}{d\eta} \right)_w \quad (2.12)$$

and the derivate of ϕ_1 replaces the derivative of T for calculating q_w .

The introduction of a heat flux potential is a frequent device in heat transfer problems, and has been applied to gases in the end wall geometry in Ref. 4. However, in this reference convection was neglected, which is equivalent to ignoring compressibility, so the density factor did not appear and ϕ became the classical potential $\int k dT$. It would appear that the omission of convection casts doubt on the validity of the work presented in Ref. 4.

We now propose to solve Eq. (2.8) by an integral method. To this end we integrate on η from $\eta = 0$ to $\eta = \infty$, remembering that $d\theta/d\eta \rightarrow 0$ as $\eta \rightarrow \infty$. The result is

$$\left(\frac{d\phi_1}{d\eta} \right)_w = \int_0^{\infty} \frac{c_p}{c_{p0}} \eta \frac{d\theta}{d\eta} d\eta = \int_{\theta_w}^1 \frac{c_p}{c_{p0}} \eta d\theta \quad (2.13)$$

This form shows that all we need to find q_w is an assumption for c_p and η as functions of Θ . Notice that Θ is now the independent variable in the integral, and the range of integration is finite. This fact is of crucial importance in the approximation scheme. The relation between c_p and Θ (or T) is given by thermodynamics. The chief question is what to use for $\eta(\Theta)$. For that we return to the differential equation (2.8) and notice that near the wall where η is small

$$\frac{d}{d\eta} \frac{d\phi_1}{d\eta} = 0, \quad \frac{d\phi_1}{d\eta} = \left(\frac{d\phi_1}{d\eta} \right)_w \quad (2.14)$$

We now choose the η profile by integrating this relation to give

$$\phi_1 - \phi_{1w} = \left(\frac{d\phi_1}{d\eta} \right)_w \eta \quad (2.15)$$

This is not a linear relation between η and Θ , but a linear relation between η and the heat flux potential, which we will see gives a power relation between η and Θ for the case where k is a power of Θ . It was for that case that the profile (2.15) was introduced by Jepsen.³

By inserting (2.15) in (2.13), using the definition of ϕ_1 in (2.11), we find the final form

$$\left(\frac{d\phi_1}{d\eta} \right)_w^2 = \int_{\Theta_w}^1 \frac{c_p}{c_{p0}} (\phi_1 - \phi_{1w}) d\Theta = \int_{\Theta_w}^1 \frac{c_p}{c_{p0}} \left(\int_{\Theta_w}^{\Theta} \frac{K}{K_0} d\Theta \right) d\Theta \quad (2.16a)$$

This is a simple quadrature formula for the heat transfer rate. In the case where c_p may be taken constant integration by parts leads to the simpler expression

$$\left(\frac{d\phi_1}{d\eta} \right)_w^2 = \int_{\Theta_w}^1 (1-\Theta) \frac{K}{K_0} d\Theta \quad (2.16b)$$

To summarize the procedure, we integrate as in the ordinary Pohlhausen method, but use the dependent variable Θ as the variable of integration. We must then insert a profile $\eta(\Theta)$. We derive the profile by evaluating the differential equation near $\eta = 0$, and integrating that expression. We note that the profile so derived does not satisfy the condition

$d\phi_1/d\eta \rightarrow 0$ as $\eta \rightarrow \infty$ which was assumed in the derivation of the integral condition (2.13). However, the profile is only used in the integral on Θ , and the error that arises is only caused by the difference between the area under the exact $\eta(\Theta)$ curve and the $(\phi_1 - \phi_{1w})/(d\phi_1/d\eta)_w$ vs Θ curve between the finite limits $\Theta = \Theta_w$ and $\Theta = 1$. Assessment of the actual error is obtained by comparison of specific cases with exact solutions.

Application to Power Law Thermal Conductivity

To investigate the accuracy of the approximate formula (2.16b) we turn to several specific cases. For a perfect gas, c_p is constant and the equation of state in the present constant pressure situation indicates that ρ is inversely proportional to T . Let us take k proportional to T^ω , a frequent representation of thermal conductivity. For convenience we also will choose the reference condition o to be the external condition e . Then Eq. (2.8) becomes

$$\frac{k}{k_e} = \Theta^\omega, \quad \frac{K}{K_e} = \Theta^{\omega-1}, \quad \frac{d}{d\eta} \left(\Theta^{\omega-1} \frac{d\Theta}{d\eta} \right) + \eta \frac{d\Theta}{d\eta} = 0 \quad (2.17)$$

and from (2.11) and (2.16b)

$$\phi_1 - \phi_{1w} = \int_{\Theta_w}^{\Theta} \Theta^{\omega-1} d\Theta = (\Theta^\omega - \Theta_w^\omega) / \omega \quad (2.18)$$

$$\left(\frac{d\phi_1}{d\eta} \right)_w^2 = \int_{\Theta_w}^1 (1-\Theta) \Theta^{\omega-1} d\Theta = \frac{1-\Theta_w^\omega}{\omega} - \frac{1-\Theta_w^{\omega+1}}{\omega+1} \quad (2.19)$$

This is the result obtained by Jepson.³ Notice that $\phi_1 \sim \Theta^\omega$, so the assumed relation between η and Θ is a linear one for η in the terms of Θ^ω , as mentioned above.

The formula (2.19) yields a finite heat transfer rate as $\Theta_w \rightarrow 0$ even for $\omega < 1$, which would not be true if a linear relation between η and Θ had been used for the profile. Another important limiting case is $\omega = 1$, which corresponds to ρk constant, for which we have

$$\left(\frac{d\phi_1}{d\eta} \right)_w^2 = \frac{(1-\Theta_w)^2}{2} = [0.707(1-\Theta_w)]^2 \quad (2.20)$$

This same expression is obtained in the limit $\Theta_w \rightarrow 1$. In both these cases an exact solution of Eq. (2.17) is possible, and yields

$$\left(\frac{d\phi_1}{d\eta}\right)_w^2 = \frac{(1-\Theta_w)^2}{\pi/2} = [0.798(1-\Theta_w)]^2 \quad (2.21)$$

A comparison of formula (2.19) with exact solutions of Eq. (2.17) is given in Table I. The exact calculations are from Jepson³ and from unpublished results obtained in the course of an investigation by Adams.⁵

TABLE I

ω	Θ_w	Approximate $(d\phi_1/d\eta)_w$ from (2.19)	Exact $(d\phi_1/d\eta)_w$	Exact/Approx.	Ref.
1/2	0	1.154	1.297	1.12	3
1/2	.0375	.975	1.080	1.11	5
1/2	.1	.850	.950	1.12	5
1/2	.5	.395	.442	1.12	3
1/2	.75	.185	.208	1.12	3
5/2	0	.338	.389	1.15	5
5/2	.0375	.338	.390	1.16	3
5/2	.1	.336	.386	1.15	3
5/2	.85	.319	.371	1.16	3
5/2	.5	.262	.298	1.14	3
5/2	.75	.154	.176	1.13	3
1	Θ_w	$(1 - \Theta_w) / \sqrt{2}$	$(1 - \Theta_w) \sqrt{2/\pi}$	$\sqrt{4/\pi} = 1.13$	
-	-1	$(1 - \Theta_w) / \sqrt{2}$	$(1 - \Theta_w) \sqrt{2/\pi}$	$\sqrt{4/\pi} = 1.13$	

We see that in all cases (2.19) yields values smaller than the exact values, but the ratio of the exact to the approximate solution is remarkably constant over a wide range of ω and Θ_w .

Another case for which exact calculations are available is one in which the k vs T curve is represented as consisting of two different power laws with a break at some temperature T_c . Adams⁵ used this form in his study of electronic heat transfer. The relation for the k curve is

$$\begin{aligned} k/k_e &= \Theta_c^{\nu-\lambda} \Theta^\lambda & \text{for } \Theta_w < \Theta < \Theta_c \\ &= \Theta^\nu & \text{for } \Theta_c < \Theta < 1 \end{aligned} \quad (2.22)$$

This leads to

$$\begin{aligned} \left(\frac{d\phi_1}{d\eta}\right)_w^2 &= \int_{\theta_w}^{\theta_c} (1-\theta) \theta_c^{\nu-\lambda} \theta^{\lambda-1} d\theta + \int_{\theta_c}^1 (1-\theta) \theta^{\nu-1} d\theta \\ &= \theta_c^{\nu-\lambda} \left\{ \left[\frac{1}{\lambda(\lambda+1)} - \frac{\theta_w^\lambda}{\lambda} + \frac{\theta_w^{\lambda+1}}{\lambda+1} \right] \right. \\ &\quad \left. + \theta_c^{\lambda-\nu} \left[\frac{1}{\nu(\nu+1)} - \frac{\theta_c^\nu}{\nu} + \frac{\theta_c^{\nu+1}}{\nu+1} \right] - \left[\frac{1}{\lambda(\lambda+1)} - \frac{\theta_c^\lambda}{\lambda} + \frac{\theta_c^{\lambda+1}}{\lambda+1} \right] \right\} \end{aligned} \quad (2.23)$$

This of course, has the same limit for $\theta_w \rightarrow 1$ as the single exponent case, Eq. (2.21).

Comparison of Eq. (2.23) with unpublished exact calculations of Adams are shown in Table II.

TABLE II

λ	ν	θ_w	θ_c	Approximate $(d\phi_1/d\eta)_w$ from (2.22)	Exact $(d\phi_1/d\eta)_w$	Exact Approx.
1/2	5/2	.222	.889	.602	.675	1.12
1/2	5/2	.167	.667	.509	.580	1.14
1/2	5/2	.125	.500	.439	.505	1.15
λ	ν	-1	-1	$(1 - \theta_w) / \sqrt{2}$	$\sqrt{2/\pi} (1 - \theta_w)$	$\sqrt{4/\pi} = 1.13$

Again we see the approximate solution (2.23) gives smaller values than the exact one, but again the ratios are very constant.

On the basis of the evidence presented in Tables I and II, it appears that multiplication by the factor $\sqrt{4/\pi}$, which makes the approximate solution agree with the exact one in the Rayleigh case $\theta_w \rightarrow 1$, gives an answer correct to within + 3% for all the numerical cases calculated. Therefore the corrected formula (2.12) for the heat transfer rate becomes (with external reference conditions)

$$-q_w = \left(\frac{\rho_e k_e c_{pe}}{2t} \right)^{1/2} T_e (1.13) \left[\int_{\theta_w}^1 (1-\theta) \frac{\rho k}{\rho_e k_e} d\theta \right]^{1/2} \quad (2.24)$$

This provides a simple and accurate formula for calculating the heat transfer rate to the end wall of a shock tube when ρ and k are given function of T , and

c_p can be taken constant. The extension to include c_p as a function of T by replacing the integral by (2.16a) has not been tested but would seem to be a reasonable guess.

It should be noted that the correction factor applied in Eq. (2.24) is equivalent to using not the profile given in (2.15) but a corrected profile

$$\phi_1 - \phi_{1w} = \frac{\pi}{4} \left(\frac{d\phi}{d\eta} \right)_w \eta \quad (2.25)$$

In Fig. 1, several $\eta(\theta)$ profiles calculated using (2.25) for the case $\rho k / \rho_e k_e = \theta^{\omega-1}$, c_p constant, are compared with the exact profiles calculated by Jépson,³ and it becomes clear why $\int \eta d\theta$ is quite accurately represented.

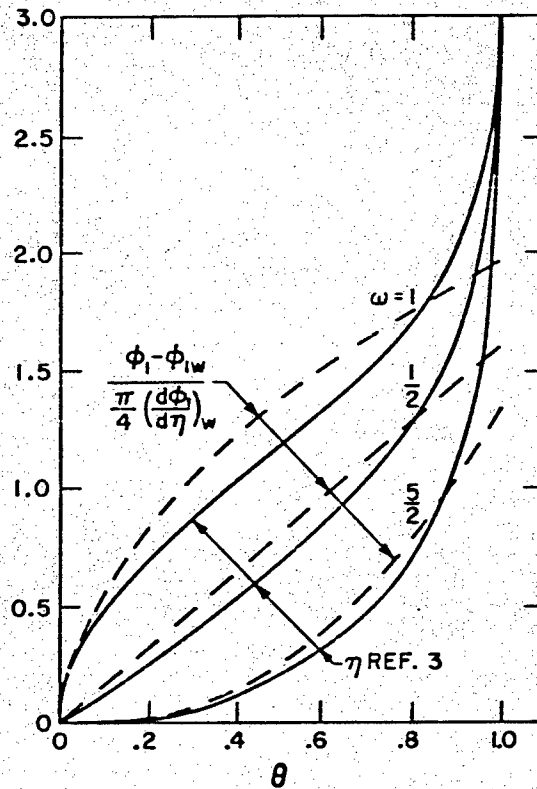


Fig. 1 Profiles of η vs θ for end wall geometry. Solid lines are the exact profiles from Ref. 3, dashed lines are the approximate profiles, Eq. (2.25).

SECTION 3

STAGNATION POINT HEAT TRANSFER

Heat transfer to the stagnation point of a blunt body has been studied intensively in recent years. It also represents a case which is exactly reducible to similarity form. Here we shall restrict ourselves to the case of a dissociating gas with Lewis number unity and flow in thermodynamic equilibrium, to illustrate the application of the method without undue complications. Under these circumstances, we have to solve the following continuity, momentum, and energy equations⁶ for the velocities u and v and the total enthalpy H :

$$\frac{\partial \rho u r^j}{\partial x} + \frac{\partial \rho v r^j}{\partial y} = 0 \quad (3.1)$$

$$\rho u \frac{\partial u}{\partial x} + \rho v \frac{\partial u}{\partial y} = -\frac{\partial p}{\partial x} + \frac{\partial}{\partial y} \left(\mu \frac{\partial u}{\partial y} \right) = \rho_e u_e \frac{\partial u_e}{\partial x} + \frac{\partial}{\partial y} \left(\mu \frac{\partial u}{\partial y} \right) \quad (3.2)$$

$$\rho u \frac{\partial H}{\partial x} + \rho v \frac{\partial H}{\partial y} = \frac{\partial}{\partial y} \left(\frac{k}{c_p} \frac{\partial H}{\partial y} \right) \quad (3.3)$$

k and c_p are the frozen thermal conductivity and specific heat of the gas. The dissipation and pressure gradient terms do not appear in the energy equation (3.3) because they are negligible at a stagnation point. The factor r^j with $j = 0$ for two-dimensional and $j = 1$ for axi-symmetric flow permits consideration of both cases at once, with r the cylindrical radius of the axi-symmetric body. Near the stagnation point $r \approx x$. These equations define the problem when combined with the boundary conditions

$$y=0: \quad u=v=0, \quad H=H_w = \text{constant} \quad (3.4)$$

$$y=\infty: \quad u=u_e, \quad H=H_e = \text{constant} \quad (3.5)$$

If the continuity equation is solved for ρv , the convective derivative operator becomes

$$\rho u \frac{\partial}{\partial x} + \rho v \frac{\partial}{\partial y} = \rho u \frac{\partial}{\partial x} - \left(r^{-j} \frac{\partial}{\partial x} \int_0^y \rho u r^j dy \right) \frac{\partial}{\partial y} \quad (3.6)$$

which eliminates v .

We now introduce the similarity variable by

$$\eta \equiv \chi_2(x) \int_0^y \rho dy \quad (3.7)$$

and assume that all quantities depend only on η . We also non-dimensionalize H and u by their external values, introducing new variables g and f by

$$H \equiv H_e g, \quad u = u_e df/d\eta \quad (3.8)$$

where H_e is the constant external enthalpy, but the external velocity u_e is a function of x . The resulting forms of the momentum and energy equations are

$$\frac{\chi_2^2}{u_e} \frac{d}{d\eta} \left(\rho \mu \frac{d^2 f}{d\eta^2} \right) + \frac{r^{-j} \chi_2}{u_e} \frac{d}{dx} \left(\frac{r^j u_e}{\chi_2} \right) f \frac{d^2 f}{d\eta^2} + \frac{1}{u_e} \frac{du_e}{dx} \left[\frac{\rho_e}{\rho} - \left(\frac{df}{d\eta} \right)^2 \right] = 0 \quad (3.9)$$

$$\frac{\chi_2^2}{u_e} \frac{d}{d\eta} \left(\frac{\rho k}{\bar{\alpha}_p} \frac{dg}{d\eta} \right) + \frac{r^{-j} \chi_2}{u_e} \frac{d}{dx} \left(\frac{r^j u_e}{\chi_2} \right) f \frac{dg}{d\eta} = 0 \quad (3.10)$$

We are now free to choose χ_2 to make the x dependence of the coefficients vanish. Then η becomes

$$\begin{aligned} \eta &= r^j \left(2 \rho_0 k_0 / \bar{\alpha}_p \right)^{-1/2} \left(\int_0^x u_e r^{2j} dx \right)^{-1/2} \int_0^y \rho dy \\ &= \left[\frac{(1+j) \bar{\alpha}_{p0}}{\rho_0 k_0} \left(\frac{du_e}{dx} \right)_{st} \right]^{1/2} \int_0^y \rho dy \end{aligned} \quad (3.11)$$

where near the stagnation point we have put $r = x$, $u_e = x(du_e/dx)_{st}$. With this choice of χ_2 , and putting $\kappa \equiv \rho k / \bar{c}_p$, the similarity equations (3.9) and (3.10) become

$$\frac{d}{d\eta} \left(\frac{\chi}{\chi_0} \sigma \frac{df}{d\eta^2} \right) + f \frac{d^2 f}{d\eta^2} + \frac{1}{1+j} \left[\frac{\rho_e}{\rho} - \left(\frac{df}{d\eta} \right)^2 \right] = 0 \quad (3.12)$$

$$\frac{d}{d\eta} \left(\frac{\chi}{\chi_0} \frac{dg}{d\eta} \right) + f \frac{dg}{d\eta} = 0 \quad (3.13)$$

while the boundary conditions (3.4) and (3.5) transform to

$$\eta=0: \quad f = df/d\eta = 0, \quad g = g_w \equiv H_w/H_e \quad (3.14)$$

$$\eta=\infty: \quad df/d\eta = g = 1 \quad (3.15)$$

Equations (3.12) and (3.13) differ slightly from the usual stagnation-point boundary layer equations,⁶ in that the Prandtl number $\sigma = \bar{c}_p \mu / k$ appears in the momentum equation instead of the energy equation. This is a consequence of choosing the quantity $\kappa \equiv \rho k / \bar{c}_p$ as the basic combination of fluid properties, rather than the more usual choice of $\rho \mu$. Since the heat transfer rather than the shear stress is of primary interest, it seems more suitable to relegate the Prandtl number to the momentum equation, which is only weakly coupled to the energy equation. The use of $\rho \mu$ is a holdover from the point of view that the momentum equation was basic and the temperature profile could be found after the velocity profile was known. For the case of constant Prandtl number, σ_0 , (3.12) and (3.13) can be put into their more familiar form by replacing η by $\sqrt{\sigma_0} \eta$ and f by $\sqrt{\sigma_0} f$.

The heat transfer rate is expressed by

$$-q_w = \left(\frac{k}{\bar{c}_p} \frac{\partial H}{\partial y} \right)_w = \frac{k_w \rho_w}{\bar{c}_{pw}} H_e \chi_2 \left(\frac{dg}{d\eta} \right)_w \quad (3.16)$$

In this case we may again define a heat flux potential ϕ_2 by inserting χ_2 from (3.11) into (3.16):

$$-q_w = \left[\frac{(1+j) \rho_0 k_0}{\bar{c}_{p0}} \left(\frac{du_e}{dx} \right)_{st} \right]^{1/2} \left(\frac{\rho k / \bar{c}_p}{\rho_0 k_0 / \bar{c}_{p0}} \frac{dg}{d\eta} \right)_w = \left[\frac{(1+j) \rho_0 k_0}{\bar{c}_{p0}} \left(\frac{du_e}{dx} \right)_{st} \right]^{1/2} \left(\frac{d\phi_2}{d\eta} \right)_w \quad (3.17)$$

The problem before us, of determining $(d\phi_2/d\eta)_w$ from Eqs. (3.12) and (3.13) plus some expressions for the fluid properties in equilibrium as a function of g , is more difficult than in the end wall geometry because of the presence in the energy equation of the stream function, f , determined by the momentum equation. A proper solution requires simultaneous consideration of both equations. However, it is well known that the influence of the momentum equation on the energy equation is small; and so we may hope to include this influence by an approximate treatment of Eq. (3.12). This will be the approach we shall take.

First consider the energy equation (3.13) and integrate from the wall to the edge of the thermal boundary layer, where $dg/d\eta = 0$. Using the definition (3.17) of ϕ_2 and integrating by parts, we find

$$\left(\frac{d\phi_2}{d\eta}\right)_w = \int_0^\infty f \frac{dg}{d\eta} d\eta = \int_{g_w}^1 f dg = \int_{g_w}^1 (1-g) \frac{df}{d\eta} \frac{d\eta}{dg} dg \quad (3.18)$$

an equation analogous to (2.13). We must now have a guess for the profiles $df(g)/d\eta$ and $\eta(g)$ just as in the end wall case we needed one for $\eta(\Theta)$. The momentum and energy equations will supply these profiles.

The f profile is determined much in the way we determined the Θ profile in the end wall case, by writing (3.12) near the wall as

$$\frac{d}{d\eta} \left(\frac{x}{x_0} \sigma \frac{d^2 f}{d\eta^2} \right) + \frac{\rho_e/\rho}{1+j} = 0 \quad (3.19)$$

We now integrate to find

$$\frac{d^2 f}{d\eta^2} = \frac{1}{\sigma} \frac{x_0}{x} \left[-\int_0^\eta \frac{\rho_e/\rho}{1+j} d\eta + A \left(\frac{d\phi_2}{d\eta} \right)_w \right] \quad (3.20a)$$

$$\frac{df}{d\eta} = \int_0^\eta \frac{x}{x_0} \left[-\int_0^\eta \frac{\rho_e/\rho}{1+j} d\eta + A \left(\frac{d\phi_2}{d\eta} \right)_w \right] \frac{d\eta}{\sigma} \quad (3.20b)$$

where A is a constant of integration, related to the shear stress, which will be evaluated later.

The $\eta(g)$ profile is obtained the same way from Eq. (3.13) near the wall:

$$\frac{d}{d\eta} \left(\frac{x}{x_0} \frac{dg}{d\eta} \right) = 0 \quad \frac{x}{x_0} \frac{dg}{d\eta} = \left(\frac{d\phi_2}{d\eta} \right)_w \quad (3.21)$$

This leads to

$$d\eta = \left(\frac{d\phi_2}{d\eta} \right)_w \frac{x}{x_0} dg \quad (3.22)$$

At this point, we must realize that we are dealing with two layers, an energy layer and a momentum layer, whose thicknesses are in general different. Outside the momentum layer, the f profile is determined from $df/d\eta = 1$, rather than Eqs. (3.20) while outside the energy layer, the g profile is $g = 1$ instead of the function of η given by Eq. (3.22). Thus, we will have to consider separately the case when the energy layer is thicker than the momentum layer and the case when the momentum layer is thicker. These relative thicknesses depend, of course, on the Prandtl number σ , and will provide one of the unknowns in the problem. Since the fluid properties depend on g only, we take that as our primary variable. Then the edge of the energy layer is specified as $g = 1$, and the location of the edge of the momentum layer is the unknown, defined as $g = g_f$ if it is thinner than the energy layer. If it is thicker than the energy layer, it will appear shortly that the distance between the edges of the two layers, $\eta_f - \eta_g$, is a convenient variable.

Before we go to the details of the two cases, let us consider the general method of solution. We have three unknowns to determine: the one of primary interest is the heat transfer parameter $(d\phi_2/d\eta)_w$; the second is the constant A in the expression for $df/d\eta$; and the third is the unknown location of the edge of the momentum layer, represented by either g_f or $\eta_f - \eta_g$, depending on whether it is thinner or thicker than the energy layer. Three conditions are therefore needed for the solution. We have available so far the energy integral equation (3.18) and the boundary condition $df/d\eta = 1$ at the edge of the momentum layer η_f (or g_f), leaving one more equation to be specified. The most symmetrical procedure for obtaining the third equation would be to treat the momentum equation exactly as the energy equation, i. e., to integrate (3.12) to the edge of the momentum layer. This can be carried through and yields a rather lengthy equation involving A and $(d\phi_2/d\eta)_w$.

algebraically and g_f transcendently in the limits of integration. However, a simpler approach to the determination of A was sought, in view of the fact that the only appearance of f is under the integral sign in Eq. (3.18) as $df/d\eta$, so only a weighted average value of $df/d\eta$ is computed. We have already imposed on $df/d\eta$ in (3.20) the condition that it vanish at the wall, and satisfied the momentum differential equation near the wall, and we will use the condition that it is unity at the edge of the momentum layer. In lieu of making it satisfy the momentum equation on the average throughout the whole momentum layer, we instead impose a second boundary condition at the edge of the layer, making*

$$\frac{d^2 f}{d\eta^2} = 0 \quad \text{at} \quad \eta = \eta_f \quad (3.23)$$

This serves as the third relation, which completes the determination of the problem. Since this condition is largely instrumental in determining A , which in turn is proportional to the shear stress, one will not expect to determine that quantity accurately. However, since $df/d\eta$ now has the correct values at $\eta = 0$ and $\eta = \eta_f$, and the correct derivative at η_f , and satisfies the correct equation near $\eta = 0$, we may hope that the effects of the momentum layer on the heat transfer are sufficiently well represented. Eventual comparison with exact solutions will provide us with the ultimate check on the usefulness of this simple approach.

With the use of the third condition (3.23) established, we may now go on to consider separately the cases of momentum layer thinner and thicker than the energy layer.

Momentum Layer Thinner Than Energy Layer (Small Prandtl Number)

The momentum layer terminates at $g = g_f < 1$. From g_f to $g = 1$, the velocity is free stream; i. e. $df/d\eta = 1$. From g_w to g_f Eqs. (3.20) are applicable. The constant A is determined, as discussed above, by letting $d^2 f/d\eta^2 = 0$ at $\eta = \eta_f$. The use of this in Eq. (3.20a) gives

$$A \left(\frac{d\phi_2}{d\eta} \right)_w^{-1} = \int_0^{\eta_f} \frac{\rho_e/\rho}{1+j} d\eta \quad (3.24)$$

We now define the integral

$$I(g) \equiv \left(\frac{d\phi_2}{d\eta} \right)_w \int_0^g \frac{\rho_e}{\rho} d\eta = \int_{g_w}^g \frac{x}{x_0} \frac{\rho_e}{\rho} dg \quad (3.25)$$

*This idea grew out of a conversation with the author's colleague, Dr. Richard Levy.

where the second form comes from using (3.22). Then (3.20b) becomes

$$\frac{df}{d\eta} = \left(\frac{d\phi_2}{d\eta}\right)_w^{-2} \frac{1}{1+j} \int_{g_w}^g (\mathbf{I}_f - \mathbf{I}) \frac{dg}{\sigma} \quad (3.26)$$

where $\mathbf{I}_f = \mathbf{I}(g_f)$ and (3.22) has been used again to replace $d\eta$.

The boundary condition $df/d\eta = 1$ at η_f (or g_f) then leads to the condition

$$\left(\frac{d\phi_2}{d\eta}\right)_w^2 = \frac{1}{1+j} \int_{g_w}^{g_f} (\mathbf{I}_f - \mathbf{I}) \frac{dg}{\sigma} \quad (3.27)$$

The basic expression (3.18) for $(d\phi_2/d\eta)_w$ can now be written in final form by breaking the range of integration at g_f and using (3.22) for $d\eta/dg$ and (3.26) for $df/d\eta$ in the lower part and (3.22) and $df/d\eta = 1$ in the upper part. The result is

$$\begin{aligned} \left(\frac{d\phi_2}{d\eta}\right)_w^4 - \left(\frac{d\phi_2}{d\eta}\right)_w^2 \int_{g_f}^1 (1-g) \frac{\kappa}{\kappa_0} dg \\ - \frac{1}{1+j} \int_{g_w}^{g_f} (1-g) \frac{\kappa}{\kappa_0} \left[\int_{g_w}^g (\mathbf{I}_f - \mathbf{I}) \frac{dg}{\sigma} \right] dg = 0 \end{aligned} \quad (3.28a)$$

If the last term is integrated by parts and (3.27) is used, this may be written

$$\begin{aligned} \left(\frac{d\phi_2}{d\eta}\right)_w^2 \left[\left(\frac{d\phi_2}{d\eta}\right)_w^2 - \int_{g_w}^1 (1-g) \frac{\kappa}{\kappa_0} dg \right] \\ + \frac{1}{1+j} \int_{g_w}^{g_f} (\mathbf{I}_f - \mathbf{I}) \left[\int_{g_w}^g (1-g) \frac{\kappa}{\kappa_0} dg \right] \frac{dg}{\sigma} = 0 \end{aligned} \quad (3.28b)$$

Equations (3.27) and (3.28) are two relations for the two unknowns $(d\phi_2/d\eta)_w$ and g_f . Once κ and σ are given as functions of g , they can be solved and the heat transfer rate determined from (3.17).

As the Prandtl number $\sigma \rightarrow 0$, the momentum layer thickness vanishes so $g_f \rightarrow g_w$. The third term of (3.28b) disappears, and the equation reduces to Eq. (2.16b) for the end wall geometry. This is the physically correct

limit for $\sigma \rightarrow 0$ because the velocity is everywhere constant at the free stream value, and changes in the x direction in the steady stagnation-point problem can be related by a constant factor to the changes in time in the unsteady end wall problem.

Momentum Layer Thicker Than Energy Layer (Large Prandtl Number)

The energy layer terminates at $\eta = \eta_g < \eta_f$. From η_g to the edge of the momentum layer, η_f , we have $g = 1$, and so the fluid properties have their external values. We can then write Eq. (3.20a) in this region.

$$\frac{d^2 f}{d\eta^2} = \frac{1}{\sigma_e} \frac{x_0}{x_e} \left[- \int_0^{\eta_g} \frac{\rho_e/\rho}{1+j} d\eta - \frac{\eta - \eta_g}{1+j} + A \left(\frac{d\phi_2}{d\eta} \right)_w^{-1} \right] \quad (3.29)$$

Applying the condition $d^2 f/d\eta^2$ at $\eta = \eta_f$, we find

$$A = (I_g + N_f)/(1+j) \quad (3.30)$$

where $I_g = I(1)$ and

$$N_f \equiv (\eta_f - \eta_g) \left(\frac{d\phi_2}{d\eta} \right)_w \quad (3.31)$$

Then in the region $\eta_g < \eta < \eta_f$, we find

$$\frac{d^2 f}{d\eta^2} = \frac{1}{\sigma_e} \frac{x_0}{x_e} \frac{\eta_f - \eta}{1+j} \quad (3.32)$$

Inside the energy layer Eq. (3.22) may be used for $d\eta$ so (3.20b) and (3.30) yield

$$\frac{df}{d\eta} = \left(\frac{d\phi_2}{d\eta} \right)_w^{-1} \frac{1}{1+j} \int_{\eta_w}^g (I_g - I + N_f) \frac{dg}{\sigma} \quad (3.33)$$

We also need the expression for $df/d\eta$ at η_f to apply a boundary condition there. This is obtained by extending the integral in Eq. (3.33) to $g = 1$, integrating (3.32) from η_g to η_f , and adding the two contributions. The result is

$$\left(\frac{df}{d\eta}\right)_f = \left(\frac{d\phi_2}{d\eta}\right)_w^{-2} \frac{1}{1+j} \left[\int_{g_w}^1 (I_g - I + N_f) \frac{dg}{\sigma} + \frac{1}{2\sigma_e} \frac{x_o}{x_e} N_f^2 \right] \quad (3.34)$$

Application of the boundary condition finally yields.

$$\left(\frac{d\phi_2}{d\eta}\right)_w^2 = \frac{1}{1+j} \left[\int_{g_w}^1 (I_g - I + N_f) \frac{dg}{\sigma} + \frac{1}{2\sigma_e} \frac{x_o}{x_e} N_f^2 \right] \quad (3.35)$$

The basic integral for $(d\phi_2/d\eta)_w$, (3.18) is now written using (3.22) for $d\eta/dg$ and (3.33) for $df/d\eta$. The result is

$$\left(\frac{d\phi_2}{d\eta}\right)_w^4 - \frac{1}{1+j} \int_{g_w}^1 (1-g) \frac{x}{x_o} \left[\int_{g_w}^g (I_g - I + N_f) \frac{dg}{\sigma} \right] dg = 0 \quad (3.36)$$

The two relations (3.35) and (3.36) determine the unknowns $(d\phi_2/d\eta)_w$ and N_f , the latter replacing g_f in the present case. Again specification of κ and σ as functions of g enable us to solve for the unknowns and thus the heat transfer by (3.17).

Application to Power Law Fluid Properties

In order to test the present approximate method, calculations have been made for constant Prandtl number σ_o , and the fluid properties have been taken as power functions of the enthalpy, with the reference condition as the edge of the energy boundary layer, i. e.,

$$\frac{x}{x_o} = \frac{\mu}{\mu_e} = \frac{\rho h / \bar{c}_p}{\rho_e h_e / \bar{c}_{pe}} = g^{\omega-1}, \quad \frac{\rho_e}{\rho} = g \quad (3.37)$$

This simple representation permits the integrals to be calculated analytically. The boundary layer equations (3.12) - (3.14) for this case become

$$\sigma_o \frac{d}{d\eta} \left(g^{\omega-1} \frac{d^2 f}{d\eta^2} \right) + f \frac{d^2 f}{d\eta^2} + \frac{1}{1+j} \left[g - \left(\frac{df}{d\eta} \right)^2 \right] = 0 \quad (3.38)$$

$$\frac{d}{d\eta} \left(g^{\omega-1} \frac{dg}{d\eta} \right) + f \frac{dg}{d\eta} = 0$$

For the first case, where the momentum layer is thinner, Eqs. (3.27) and (3.28a) become

$$\left(\frac{d\phi_2}{d\eta}\right)_w^2 = \frac{1}{(1+j)\sigma_0} \left[I_{\omega+2}^f - g_w I_{\omega+1}^f \right]$$

(3.39a)

$$\left(\frac{d\phi_2}{d\eta}\right)_w^4 - \left(\frac{d\phi_2}{d\eta}\right)_w^2 \left[\frac{1-g_f^\omega}{\omega} - \frac{1-g_f^{\omega+1}}{\omega+1} \right]$$

$$\frac{-1}{(1+j)\sigma_0} \left[\frac{g_f^{\omega+1}}{\omega+1} (I_{\omega+1}^f - I_{\omega+2}^f) - \frac{I_{2\omega+2}^f - I_{2\omega+3}^f}{(\omega+1)(\omega+2)} \right.$$

$$\left. + \left(\frac{g_w}{\omega+2} - g_w g_f^{\omega+1} \right) \frac{I_{\omega}^f - I_{\omega+1}^f}{\omega+1} \right] = 0$$

(3.39b)

where

$$I_n^f \equiv \int_{g_w}^{g_f} g^{n-1} dg = (g_f^n - g_w^n)/n$$

(3.40)

To verify the approach to the end wall result as $\sigma_0 \rightarrow 0$, (i.e., $g_f \rightarrow g_w$), we may write (3.39b) in the form corresponding to (3.28b) and then divide by (3.39a). The result is

$$\left(\frac{d\phi_2}{d\eta}\right)_w^2 - \left[\frac{1-g_w^\omega}{\omega} - \frac{1-g_w^{\omega+1}}{\omega+1} \right] + \left[I_{\omega+2}^f - g_w I_{\omega+1}^f \right]^{-1}$$

$$\times \left[\frac{g_f^{\omega+2}}{\omega+2} (I_{\omega}^f - I_{\omega+1}^f) - \frac{g_f^{\omega+1}}{\omega+1} (I_{\omega+1}^f - I_{\omega+2}^f) + \frac{I_{2\omega+2}^f - I_{2\omega+3}^f}{(\omega+1)(\omega+2)} \right] = 0 \quad (3.39c)$$

Only the last term involves g_f and therefore σ_0 . It is easy to show that as $g_f \rightarrow g_w$ the last term is of order $g_f - g_w$ for $g_w \neq 0$ and g_f^ω for $g_w = 0$. Thus the last term vanishes as $\sigma_0 \rightarrow 0$ and we recover the end wall result Eq. (2.19).

For the second case, where the momentum layer is thicker, Eqs. (3.35) and (3.36) become

$$\left(\frac{d\phi_2}{d\eta}\right)_w^2 = \frac{1}{(1+j)\sigma_0} \left[I_{\omega+2}^g - g_w I_{\omega+1}^g + (1-g_w)N_f + \frac{1}{2}N_f^2 \right] \quad (3.41a)$$

$$\begin{aligned} \left(\frac{d\phi_2}{d\eta}\right)_w^4 - \frac{1}{(1+j)\sigma_0} \left[\frac{I_{\omega+1}^g - I_{\omega+2}^g}{\omega+1} - \frac{I_{2\omega+2}^g - I_{2\omega+3}^g}{(\omega+1)(\omega+2)} \right. \\ \left. + \left(\frac{g_w^{\omega+2}}{\omega+2} - g_w\right) \frac{I_{\omega}^g - I_{\omega+1}^g}{\omega+1} + \frac{N_f}{\omega+1} (I_{\omega+2}^g - g_w I_{\omega}^g) \right] = 0 \end{aligned} \quad (3.41b)$$

where

$$I_n^g = \int_{g_w}^1 g^{n-1} dg = (1 - g_w^n)/n \quad (3.42)$$

For a given set of values g_w , ω , σ_0 and j ($=0$ or 1), one must solve either Eqs. (3.39) for g_f and $(d\phi_2/d\eta)_w$ or Eqs. (3.41) for N and $(d\phi_2/d\eta)_w$. By their definitions, we must have $g_w < g_f < 1$ and $N_f > 0$, and this restriction has in all cases so far calculated been sufficient to provide a unique solution. The relative size of the momentum and energy layers is therefore determined after the solution is obtained.

One feature of the solutions immediately apparent is that j and σ_0 (the pressure gradient parameter and Prandtl number) appear only in combination and never separately. This is a direct consequence of using the simplified condition (3.26) to determine A . If the actual momentum integral were used, σ_0 and j would also appear separately. To the author's knowledge, the fact that j and σ_0 can be combined into a single parameter has not previously been suggested, and the only exact calculations extensive enough to test it are the $\mu k/c_p = \text{constant}$ ones of Squire,⁷ Subulkin,⁸ and Cohen and Reshotko.^{9,10} From the results of these references, and some extensions of them, $(d\phi_2/d\eta)_w/(1-g_w)$ is plotted in Fig. 2 against $(1+j)^{-1}\sigma_0^{-1}$ for $g_w = 0, 1$. For each g_w , the correlation is seen to be quite good, thus lending some support to the present approximate theory even before any calculations are made.

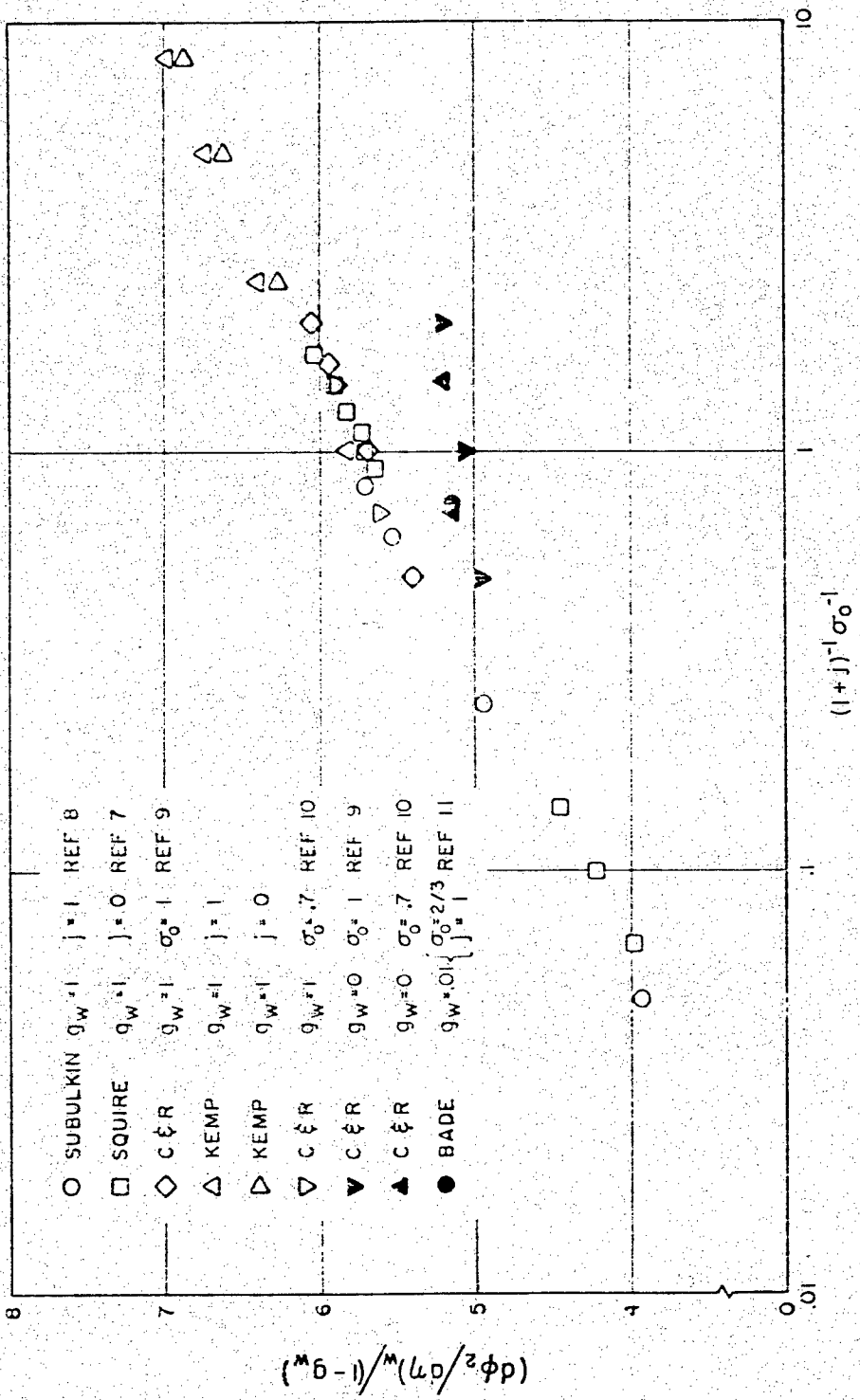


Fig. 2 Correlation of exact heat transfer calculation with the parameter $(1+j)^{-1}\sigma_0^{-1}$.

Special Cases

Before proceeding to describe the numerical solutions of the three parameter system, several important special cases will be discussed.

In the special case $\omega = 1$, which corresponds to $\kappa = \rho k / \bar{c}_p$ constant (or $\rho\mu$ constant), Eqs. (3.39) and (3.41) become

$$\left(\frac{d\phi_2}{d\eta}\right)_\omega^2 = \frac{(g_f - g_w)^2}{2(1+j)\sigma_0} \left(\frac{2g_f + g_w}{3}\right) \quad (3.43a)$$

$$\begin{aligned} & \left(\frac{d\phi_2}{d\eta}\right)_\omega^4 - \left(\frac{d\phi_2}{d\eta}\right)_\omega^2 (1-g_w)^2 \left(\frac{g_f - g_w}{1-g_w} - 1\right)^2 \\ & - \frac{(1-g_w)^4}{(1+j)\sigma_0} \left(\frac{g_f - g_w}{1-g_w}\right)^3 \left[\frac{5g_f + 3g_w}{24} - \frac{g_f - g_w}{1-g_w} \left(\frac{3g_w}{40} + \frac{2g_f}{15}\right) \right] = 0 \end{aligned} \quad (3.43b)$$

$$\left(\frac{d\phi_2}{d\eta}\right)_\omega^2 = \frac{(1-g_w)^2}{2(1+j)\sigma_0} \left[\left(1 + \frac{N_f}{1-g_w}\right)^2 - \frac{1-g_w}{3} \right] \quad (3.44a)$$

$$\left(\frac{d\phi_2}{d\eta}\right)_\omega^4 - \frac{(1-g_w)^4}{(1+j)\sigma_0} \left[\frac{1}{6} \left(1 + \frac{N_f}{1-g_w}\right) - \frac{1}{24} - \frac{1-g_w}{20} \right] = 0 \quad (3.44b)$$

which can be reduced to quartic equations for g_f and N_f .

In the incompressible limit $g_w \rightarrow 1$, which can be derived from the above equations, since the value of ω does not enter the problem in this limit, (3.43a) becomes

$$g_w \rightarrow 1: \left(\frac{1}{1-g_w} \frac{d\phi_z}{d\eta} \right)_w^2 = \frac{1}{2(1+j)\sigma_0} \left(\frac{g_f - g_w}{1-g_w} \right)^2 \quad (3.45a)$$

and when this is combined with the limit of (3.43b), a quadratic equation results whose relevant solution is

$$g_w \rightarrow 1: \frac{g_f - g_w}{1-g_w} = \frac{-\frac{1}{3} + \left[\frac{1}{9} + \frac{1}{(1+j)\sigma_0} - \frac{1}{6} \right]^{1/2}}{\frac{1}{(1+j)\sigma_0} - \frac{1}{6}} \quad (3.45b)$$

Equations (3.45) provide an explicit formula for the heat transfer in the incompressible, low Prandtl number case. From Eq. (3.45b) and its derivative, one can show that the required physical limitation that $0 \leq (g_f - g_w)/(1 - g_w) \leq 1$ (which required elimination of the other root of the quadratic) is satisfied only for $0 \leq (1+j)\sigma_0 \leq 2$, giving the range of Prandtl number for which Eqs. (3.45) are applicable. For larger values, the momentum layer is thicker than the energy layer in the present theory, and Eqs. (3.44) can be written

$$\left(\frac{1}{1-g_w} \frac{d\phi_z}{d\eta} \right)_w^2 = \frac{1}{2(1+j)\sigma_0} \left(1 + \frac{N_f}{1-g_w} \right)^2 \quad (3.46a)$$

$g_w \rightarrow 1$:

$$\frac{1}{(1+j)\sigma_0} \left(1 + \frac{N_f}{1-g_w} \right)^4 - \frac{2}{3} \left(1 + \frac{N_f}{1-g_w} \right) + \frac{1}{6} = 0 \quad (3.46b)$$

Calculation of the heat transfer in this incompressible, high Prandtl number case requires solution of the simple quartic equation (3.46b).

By examining the left side of (3.46b) and its derivative, it can be verified that the required limitation $N_f/(1 - g_w) \geq 0$ here provides a solution only for $(1 + j)\sigma_0 \geq 2$. One can also see that at the critical value $(1 + j)\sigma_0 = 2$, the left side of (3.46b) changes sign, thus verifying in this simple case the numerical criterion to be described below for deciding which set of equations will provide the solution for a given value of $(1 + j)\sigma_0$.

We have already pointed out that in the limit $\sigma_0 \rightarrow 0$, Eqs. (3.39) reduce to the proper results, namely the end wall case considered previously. The opposite limit $\sigma_0 \rightarrow \infty$ can also be derived easily. The appropriate starting point is Eqs. (3.41), since the momentum layer will be thicker than the energy layer. Eqs. (3.41) indicate two possibilities as $\sigma_0 \rightarrow \infty$. One is that N_f remain finite, in which case $(d\phi_2/d\eta)_w$ becomes zero and the quantity in curly brackets in (3.41b) must vanish. In the limits $\omega = 1$ and $g_w = 1$, this leads to $N_f < 0$, an unacceptable solution; so it probably is unacceptable in the general case also. The other possibility is the more reasonable one, that the momentum layer thickness represented by N_f approaches infinity. With this assumption, only the N_f^2 term on the right of (3.41a) and the first term and N_f term in (3.41b) are important and a simple calculation gives

$$\sigma_0 \rightarrow \infty: \left(\frac{d\phi_2}{d\eta} \right)_w \rightarrow \left[\frac{1}{\omega+1} \left(\frac{1-g_w^{\omega+2}}{\omega+2} - g_w \frac{1-g_w^\omega}{\omega} \right) \right]^{1/3} \left[\frac{2}{(1+j)\sigma_0} \right]^{1/6} \quad (3.47)$$

This is an asymptotic expression for the heat transfer rate parameter in the general case. It is well known that as $\sigma_0 \rightarrow \infty$, the Prandtl number dependence of the temperature gradient is $\sigma_0^{1/3}$. Equation (3.47) is in agreement with this when we recall that the present definition of η differs from the usual definition and to convert to the latter, one must imagine the right side of (3.47) multiplied by $\sqrt{\sigma_0}$.

The cases $\omega = 1$ and $g_w = 1$ both lead to the same expression

$$\begin{aligned} \sigma_0 \rightarrow \infty: \\ g_w \rightarrow 1: \end{aligned} \left(\frac{d\phi_2}{d\eta} \right)_w \rightarrow \frac{1-g_w}{6^{1/3}} \left[\frac{2}{(1+j)\sigma_0} \right]^{1/6} \quad (3.48)$$

One can argue that both these cases should have the same limit. They have the same energy equation and differ only in the factor g instead of unity in the pressure gradient term in the momentum equation. But in this limit, the momentum layer is so much thicker than the energy layer that it sees a constant temperature flow at the external temperature, so $g = 1$. Thus the $g_w = 1$ and $\omega = 1$ cases satisfy the same equations and so have the same expression for heat transfer. For more general cases, where ω appears explicitly in the energy equation, one would expect both ω and g_w to appear in the limiting value, as they do in Eq. (3.47).

Merk¹² has given an exact asymptotic expression for the case $g_w = 1$, which should also be valid for the case $\omega = 1$, according to the argument just given. In the present notation, Merk's result is

$$\begin{matrix} \sigma_0 \rightarrow \infty : \\ g_w \rightarrow 1 : \end{matrix} \left(\frac{d\phi_2}{d\eta} \right)_w \rightarrow \frac{1-g_w}{6^{1/3}} \frac{1}{\sigma_0^{1/3}} \frac{1}{0.893} \left[\frac{1}{\sqrt{\sigma_0}} \frac{d^2 f}{d\eta^2} \right]_w^{1/3} \quad (3.49)$$

The last bracket contains the wall shear stress parameter, which is independent of σ_0 in this case. Comparison between (3.48) and (3.49) will be given later. The author has been unable to find a comparable exact formula for $\omega \neq 1$, $g_w \neq 1$, so Eq. (3.47) represents an otherwise unavailable expression for the case of cooled walls with $\rho k / \bar{c}_p$ not constant.

Numerical Solutions and Comparisons with Exact Solutions

We will now proceed to the actual numerical solution of Eqs. (3.39) and (3.41). This is best done on a digital computer, since Eqs. (3.39) are transcendental in g_f , while Eqs. (3.41) can be reduced to a quartic in $(d\phi_2/d\eta)_w^2$ or N_f . The advantage in using the approximate method over actually integrating the exact differential equations (3.38) is in the considerable saving in computing time. The approximate method requires only the iterative solution of transcendental or quartic equations, while the exact solution requires integration of a two-point boundary-value problem, with a number of integrations to $\eta \gg 1$ usually necessary before the outer boundary condition is satisfied.

The procedure used to obtain a solution was the following. The value $g_f = 1$ was used in (3.39a) to obtain a value of $(d\phi_2/d\eta)_w$; this was inserted into the left side of (3.39b) together with $g_f = 1$. If the left side of (3.39b) was positive with these values, a new guess for $g_f < 1$ was made, and the procedure repeated until (3.39b) was satisfied, which always occurred for $g_w < g_f < 1$. If the left side of (3.39b) was negative for $g_f > 1$, attention was shifted to Eqs. (3.41), which were then solved by iteration, starting at $N_f = 0$ and searching through increasing values of N_f . This method has produced a solution in all cases attempted so far and was verified analytically in the discussion of the limiting case $g_w = 1$ given above.

To compare the solutions of the present approximate theory with exact solutions of Eqs. (3.38), use may again be made of the results of Refs. 8, 9, and 10 as well as recent work of Bade.¹¹ Such a comparison is shown in Table III. Where no reference is given, the integration of the exact equations was done by the author.

TABLE III

j	σ_0	$(1+j)\sigma_0$	ω	K_W	Approx. $(d\sigma_0/d\eta)_W$	Exact $(d\sigma_0/d\eta)_W$	Exact/Approx.	Ref.
1	2/3	4/3	.9	.01	.495	.531	1.07	11
1	2/3	4/3	.9	.80	.104	.112	1.08	11
1	2/3	4/3	.8	.01	.517	.556	1.07	11
1	2/3	4/3	.8	.80	.105	.111	1.07	11
1	2/3	4/3	.7	.01	.541	.585	1.08	11
1	2/3	4/3	.7	.80	.105	.113	1.08	11
1	2/3	4/3	.6	.01	.595	.646	1.09	11
1	2/3	4/3	.6	.80	.106	.115	1.08	11
1	1	2	1	0	.460	.495	1.08	9
1	.7	1.4	1	0	.477	.513	1.07	10
j	0	0	1	K_W	.707(1- K_W)	.798(1- K_W)	1.13	Table I
1	.71	1.42	.605	.4	.323	.348	1.07	
1	.71	1.42	.590	.0123	.504	.611	1.08	
1	∞	∞	2	$\rightarrow 1$.550(1- K_W) $\sigma_0 - 1/6$.601(1- K_W) $\sigma_0 - 1/6$	1.09	Eqs. (3, 48, 9)
1	10	20	∞	$\rightarrow 1$.361(1- K_W)	.393(1- K_W)	1.09	8
1	2	4	∞	$\rightarrow 1$.456(1- K_W)	.494(1- K_W)	1.08	8
1	1	2	∞	$\rightarrow 1$.500(1- K_W)	.539(1- K_W)	1.08	8
1	.6	1.2	∞	$\rightarrow 1$.530(1- K_W)	.571(1- K_W)	1.08	8
1	.1	0.2	∞	$\rightarrow 1$.620(1- K_W)	.674(1- K_W)	1.09	
1	.06	0.12	∞	$\rightarrow 1$.632(1- K_W)	.698(1- K_W)	1.10	
1	.01	0.02	∞	$\rightarrow 1$.675(1- K_W)	.751(1- K_W)	1.11	
j	0	0	∞	$\rightarrow 1$.707(1- K_W)	.798(1- K_W)	1.13	Table I
0	1	1	1	0	.493	.506	1.03	10
0	.7	0.7	1	0	.510	.521	1.02	10
0	∞	∞	∞	$\rightarrow 1$.619(1- K_W) $\sigma_0 - 1/6$.661(1- K_W) $\sigma_0 - 1/6$	1.07	Eqs. (3, 48, 9)
0	15	.15	∞	$\rightarrow 1$.376(1- K_W)	.398(1- K_W)	1.06	9
0	1	1	∞	$\rightarrow 1$.541(1- K_W)	.572(1- K_W)	1.06	8
0	.7	0.7	∞	$\rightarrow 1$.560(1- K_W)	.591(1- K_W)	1.06	10

Table III shows the same striking result as Tables I and II, namely the small percentage variation in the ratio of exact to approximate values of $(d\phi_2/d\eta)_w$. If one restricts oneself to values of $(1+j)\sigma_0 > 0.1$, the variation is from 1.02 to 1.10, or a +4% variation about 1.06. Thus a suitable correction factor in this range is 1.06. To make this fair smoothly into the factor 1.13 suggested for the end wall case ($\sigma_0 = 0$), one can add a term which is negligible for $(1+j)\sigma_0 > 0.1$ but approaches 0.07 as $\sigma_0 = 0$. A suitable correction factor which fulfills these requirements is $1.06 + 0.07 \exp[-10(1+j)\sigma_0]$. Use of this factor changes the heat transfer relation (3.17) to

$$-q_w = \left[\frac{(1+j)\rho_e k_e}{\bar{\tau}_{pe}} \left(\frac{du_e}{dx_{st}} \right) \right]^{1/2} \left\{ [1.06 + 0.07 e^{-10(1+j)\sigma_0}] \left(\frac{d\phi_2}{d\eta} \right)_w \right\} \quad (3.50)$$

which has a maximum error of +4% for all the cases in Table III. Use of this formula with the present approximate method of solution of the stagnation-point boundary-layer equations yields an accurate prediction of heat transfer rate for power law fluid properties and constant Prandtl number. The necessary computing time is several factors of ten less than that required to solve the exact two-point boundary-value problem.

SECTION 4

CONCLUSIONS

A simple integral method has been suggested for calculation of heat transfer rate from similarity boundary layer equations. The method has been applied to the end wall of a shock tube behind a reflected shock (Rayleigh-type problem) for a perfect gas and to the stagnation point for a gas in thermodynamic equilibrium with Lewis number unity. In both cases explicit expressions were derived when the thermal conductivity, density, and specific heat were expressed as powers of the temperature or enthalpy, and the Prandtl number was constant.

For the end wall geometry, a simple analytical expression for the heat transfer was obtained and compared with exact calculations. A constant correction factor brought the formula into agreement with the exact results within $\pm 3\%$ for a large range of powers and wall to stream temperature ratios. The expression for the heat transfer rate is

$$-q_w = \left(\frac{\rho_e k_e c_{pe}}{2t} \right)^{1/2} T_e \left[1.13 \left(\frac{d\phi_1}{d\eta} \right)_w \right] \quad (4.1)$$

where $(d\phi_1/d\eta)_w$ is obtained from Eq. (2.16a). In the case $k \propto T^\omega$, c_p constant, Eq. (2.19) gives an explicit formula for $(d\phi_1/d\eta)_w$ already obtained by Jepson.³ In the case where k is proportional to two different powers of T in different temperature ranges, $(d\phi_1/d\eta)_w$ is found from Eq. (2.23). The same correction factor (1.13) holds for both cases and presumably for any linear combination of power laws.

For the stagnation point geometry, two pair of transcendental equations (3.39) and (3.41) were derived, one pair of which in any given case provides the solution for the heat transfer parameter and relative size of the momentum and energy layers. The two pair of equations must be considered together, since one is appropriate when the momentum layer is thinner than the energy layer, the other appropriate in the reverse situation. Machine solution of these equations by trial and error is many times faster than solution of the exact differential equations. A feature of the approximate equations is that the Prandtl number and pressure gradient parameter only appear together as one parameter. In the only case known to the author where exact calculations cover an extensive enough range of these two parameters to permit testing this result, namely the case $\rho k / \bar{c}_p = \text{constant}$, the single

parameter correlated the heat transfer rate within a few percent.

When the results of the approximate stagnation point calculations for power law fluid properties and constant Prandtl number were compared to exact values, a correction factor was found which brought agreement within $\pm 4\%$. The heat transfer rate given by the approximate theory is

$$-q_w = \left[\frac{(1+j) \rho_e k_e}{\tau_{pe}} \left(\frac{du_e}{dx} \right)_{st} \right]^{1/2} \left\{ [1.06 + 0.07 e^{-10(1+j)\sigma_0}] \left(\frac{d\phi_2}{d\eta} \right)_w \right\} \quad (4.2)$$

where $(d\phi_2/d\eta)_w$ is obtained by solving the appropriate pair of Eqs. (3.39) or (3.41).

REFERENCES

1. Schlichting, H., "Boundary Layer Theory," Chapter XII, McGraw-Hill, New York, 1955.
2. Bush, W. B., "A Method of Obtaining an Approximate Solution of the Laminar Boundary-Layer Equations," J. Aerospace Sci., Vol. 28, No. 4, pp. 350-351, April 1961.
3. Jepson, B-M., "Heat Transfer in a Completely Ionized Gas," Magneto-hydrodynamics Laboratory, Department of Mechanical Engineering, Massachusetts Institute of Technology, Report No. 61-7, AFOSR 1562, July 1961.
4. Hansen, C. F., Early, R. A., Alzofon, F. E., and Witteborn, F. C., "Theoretical and Experimental Investigation of Heat Conduction in Air, Including Effects of Oxygen Dissociation," NASA Technical Report R-27, (1959). See also Hansen, C. F., "Heat Diffusion in Gases, Including Effects of Chemical Reaction," ARS Journal, Vol. 30, No. 10, pp. 942-946, October 1960.
5. Adams, M. C., "A Look at the Heat Transfer Problem at Super Satellite Speeds," Avco-Everett Research Laboratory AMP 53, December 1960. Also American Rocket Society Report 1556-60.
6. Fay, J. A., and Riddell, F. R., "Theory of Stagnation Point Heat Transfer in Dissociated Air," J. Aero. Sci., Vol. 25, No. 2, pp. 73-85, February 1958.
7. Goldstein, S., "Modern Developments in Fluid Dynamics," Vol. II, pp. 631-632, Oxford, (1938).
8. Subulkin, M., "Heat Transfer Near the Forward Stagnation Point of a Body of Revolution," J. Aero. Sci., Vol. 19, No. 8, pp. 570-571, August 1952.
9. Cohen, C. B., and Reshotko, E., "Similar Solutions for the Compressible Laminar Boundary Layer with Heat Transfer and Pressure Gradient," NACA Report 1293, (1956). (Supersedes TN 3325)
10. Cohen, C. B., and Reshotko, E., "The Compressible Laminar Boundary Layer with Heat Transfer and Arbitrary Pressure Gradient," NACA Report 1294, (1956). (Supersedes TN 3326)

11. Bade, W. L., "Stagnation Point Heat Transfer in a High-Temperature Inert Gas," Physics of Fluids, Vol. 5, No. 2, pp. 150-154, February 1962.
12. Merk, H. J., "Rapid Calculations for Boundary-Layer Transfer Using Wedge Solutions and Asymptotic Expansion," J. Fluid Mechanics, Vol. 5, Pt. 3, p. 470, April 1959.

<p>UNCLASSIFIED</p> <p>Heat Transfer Rates - Calculation.</p> <ol style="list-style-type: none"> Differential Equations. Shock Tubes - Applications. Boundary Layer Equations. <p>I. Title.</p> <p>II. Kemp, Nelson H.</p> <p>III. Avco-Everett Research Report 137.</p> <p>IV. BSD - TDR - 62 - 171.</p> <p>V. Contract AF 04(694) - 33.</p> <p>UNCLASSIFIED</p>	<p>Avco-Everett Research Laboratory, Everett, Massachusetts</p> <p>CALCULATION OF HEAT TRANSFER FROM SIMILARITY BOUNDARY LAYER EQUATIONS BY A SIMPLE INTEGRAL METHOD, by Nelson H. Kemp, June 1962, 32 p., incl. illus. (Avco-Everett Research Report 137; BSD - TDR - 62 - 171) (Contract AF 04(694) - 33)</p> <p>Unclassified</p> <p>A simple integral method is developed for calculation of the heat transfer rate from similarity boundary layer equations with arbitrary variation of fluid properties. The method is applied to the end wall of a shock tube behind a reflected shock in a perfect gas, and to the stagnation point for a gas in thermodynamic equilibrium with Lewis number unity. Explicit formulas and results are obtained when the fluid properties are powers of the enthalpy or temperature, and Prandtl number is constant. For the end wall geometry, an analytical expression for the heat transfer rate is derived which can be correlated with exact calculations within $\pm 3\%$ for all cases compared. For the stagnation point geometry</p> <p>(over)</p>	<p>UNCLASSIFIED</p> <p>Heat Transfer Rates - Calculation.</p> <ol style="list-style-type: none"> Differential Equations. Shock Tubes - Applications. Boundary Layer Equations. <p>I. Title.</p> <p>II. Kemp, Nelson H.</p> <p>III. Avco-Everett Research Report 137.</p> <p>IV. BSD - TDR - 62 - 171.</p> <p>V. Contract AF 04(694) - 33.</p> <p>UNCLASSIFIED</p>	<p>Avco-Everett Research Laboratory, Everett, Massachusetts</p> <p>CALCULATION OF HEAT TRANSFER FROM SIMILARITY BOUNDARY LAYER EQUATIONS BY A SIMPLE INTEGRAL METHOD, by Nelson H. Kemp, June 1962, 32 p., incl. illus. (Avco-Everett Research Report 137; BSD - TDR - 62 - 171) (Contract AF 04(694) - 33)</p> <p>Unclassified</p> <p>A simple integral method is developed for calculation of the heat transfer rate from similarity boundary layer equations with arbitrary variation of fluid properties. The method is applied to the end wall of a shock tube behind a reflected shock in a perfect gas, and to the stagnation point for a gas in thermodynamic equilibrium with Lewis number unity. Explicit formulas and results are obtained when the fluid properties are powers of the enthalpy or temperature, and Prandtl number is constant. For the end wall geometry, an analytical expression for the heat transfer rate is derived which can be correlated with exact calculations within $\pm 3\%$ for all cases compared. For the stagnation point geometry</p> <p>(over)</p>
<p>UNCLASSIFIED</p> <p>Heat Transfer Rates - Calculation.</p> <ol style="list-style-type: none"> Differential Equations. Shock Tubes - Applications. Boundary Layer Equations. <p>I. Title.</p> <p>II. Kemp, Nelson H.</p> <p>III. Avco-Everett Research Report 137.</p> <p>IV. BSD - TDR - 62 - 171.</p> <p>V. Contract AF 04(694) - 33.</p> <p>UNCLASSIFIED</p>	<p>two pair of transcendental algebraic equations are obtained, one pair of which gives the heat transfer rate when the momentum layer is thinner than the energy layer, the other pair when it is thicker. Numerical solutions of these equations, requiring much less computing time than integration of the exact differential equations, can be correlated with exact solutions to within $\pm 4\%$. The integral method indicates the pressure gradient parameter and Prandtl number can be combined into only one parameter, and examination of results of exact calculations shows this correlation to be quite accurate.</p>	<p>UNCLASSIFIED</p> <p>Heat Transfer Rates - Calculation.</p> <ol style="list-style-type: none"> Differential Equations. Shock Tubes - Applications. Boundary Layer Equations. <p>I. Title.</p> <p>II. Kemp, Nelson H.</p> <p>III. Avco-Everett Research Report 137.</p> <p>IV. BSD - TDR - 62 - 171.</p> <p>V. Contract AF 04(694) - 33.</p> <p>UNCLASSIFIED</p>	<p>two pair of transcendental algebraic equations are obtained, one pair of which gives the heat transfer rate when the momentum layer is thinner than the energy layer, the other pair when it is thicker. Numerical solutions of these equations, requiring much less computing time than integration of the exact differential equations, can be correlated with exact solutions to within $\pm 4\%$. The integral method indicates the pressure gradient parameter and Prandtl number can be combined into only one parameter, and examination of results of exact calculations shows this correlation to be quite accurate.</p>